

**1 The Influence of the Quasi-Biennial Oscillation on**  
**2 the North Pacific and El-Niño teleconnections**

C. I. Garfinkel,<sup>1</sup> D. L. Hartmann,<sup>1</sup>

---

C. I. Garfinkel, Department of Atmospheric Science, University of Washington, Seattle, WA  
98195, USA. (cig4@atmos.washington.edu)

D. L. Hartmann, Department of Atmospheric Science, University of Washington, Seattle, WA  
98195, USA

<sup>1</sup>Department of Atmospheric Science,  
University of Washington, Seattle, WA,  
USA.

3 **Abstract.** Reanalysis and model data are used to study El-Niño South-  
4 ern Oscillation(ENSO) teleconnections in the North Pacific during boreal win-  
5 ter. El-Niño events appear to have a significantly stronger teleconnection when  
6 the equatorial stratospheric Quasi-Biennial Oscillation (QBO) is in its west-  
7 erly phase relative to its easterly phase at 70hPa in both the reanalysis record  
8 and in the Whole Atmosphere Community Climate Model (WACCM). The  
9 difference is much larger in the reanalysis, however. Composites of easterly  
10 QBO at 70hPa show an anomalous ridge over the North Pacific, which ex-  
11 plains part of the weakening of El-Niño teleconnections. Associated with this  
12 ridge are easterly anomalies at the climatological subtropical jet position and  
13 westerly anomalies in the deep tropics. A shallow water model linearized about  
14 such zonal wind anomalies gives a weaker extratropical response to a deep  
15 tropical vorticity anomaly, suggesting a dynamical explanation of how the  
16 QBO can influence the extratropical response to anomalous ENSO convec-  
17 tion. These results suggest that modification of wave propagation is likely  
18 an important cause of the observed differences in El-Niño teleconnections be-  
19 tween easterly and westerly QBO phases, but sampling variability and dif-  
20 ferences in underlying tropical convection are also likely contributors.

## 1. Introduction

21 Over the past decade much evidence has accumulated that stratospheric anomalies can  
22 affect the wintertime tropospheric circulation. In particular, anomalies of the stratospheric  
23 polar vortex have been shown to affect the Northern Annular Mode (NAM) down to the  
24 surface[Baldwin and Dunkerton, 1999; Polvani and Kushner, 2002; Limpasuvan et al.,  
25 2004]. Even though the equatorial stratospheric QBO is the dominant mode of inter-  
26 annual stratospheric variability in the Tropics, its affect on the wintertime tropospheric  
27 circulation has been less thoroughly investigated.

28 A first possible pathway for the QBO to affect the troposphere is through its effect  
29 on the polar vortex [Holton and Tan, 1980; Baldwin et al., 2001; Coughlin and Tung,  
30 2001; Ruzmaikin et al., 2005]. Once the QBO influences the vortex, it could affect the  
31 troposphere just like any vortex anomaly [Baldwin and Dunkerton, 1999; Limpasuvan  
32 et al., 2004]. This pathway seems particularly evident in the North Atlantic [Boer and  
33 Hamilton, 2008] but much less so elsewhere. A second possible pathway is a direct effect of  
34 the QBO on the tropical or subtropical troposphere. Crooks and Gray [2005] and Haigh  
35 et al. [2005] find that the anomalous QBO winds seemingly curve downwards into the  
36 troposphere in a horseshoe shaped pattern, with easterlies in the deep Tropics, westerlies  
37 in the subtropics, and easterlies in the extratropics during WQBO. How this signal is  
38 communicated downwards through the tropopause has not been fully explained, however.  
39 Collimore et al. [2003] connect anomalies in convection with the stratospheric QBO. If such  
40 convective anomalies exist, they could affect the extratropics as well, as Ho et al. [2009]

41 found for summertime tropical cyclone tracks in the western North Pacific Ocean(hereafter  
42 NP).

43 Much has been written on El-Niño (hereafter EN) teleconnections into the extratropics.  
44 Hoskins and Karoly [1981] demonstrate how a Rossby wave train launched by EN related  
45 anomalous vorticity can reach the NP and Canada. Numerous papers have subsequently  
46 elaborated on this wave propagation theory. Simmons et al. [1983] find that a NP anomaly  
47 can grow in a zonally asymmetric basic state by extracting energy from the mean flow, and  
48 thus can be excited without tropical convection; Sardeshmukh and Hoskins [1988] show  
49 how linearizing about a divergent basic state affects the Rossby wave source term; and  
50 Held et al. [1989] discuss the importance of subtropical convergence that is forced, in large  
51 part, by anomalous extratropical transients. Branstator [1992] finds that the momentum  
52 flux associated with transients with time scales shorter than seven days, the underlying  
53 thermal forcing, and the zonally asymmetric climatological state, are all essential for the  
54 maintenance of long lived NP anomalies. Ting and Sardeshmukh [1993] find that slight  
55 differences in the ambient flow lead to very different low frequency modes and thus to  
56 very different responses to tropical perturbations (in particular, the ambient flow with  
57 a stronger Pacific subtropical jet gave a stronger response, a finding we will confirm).  
58 Feldstein [2002] and Franzke and Feldstein [2005] find that NP growth is heavily influenced  
59 by the zonally asymmetric climatological mean state. All of this evidence indicates that  
60 EN teleconnections are affected by variability outside of the deep tropical Pacific.

61 EN's observed teleconnection in the NP has differed depending on the state of the QBO  
62 at 50hPa[Garfinkel and Hartmann, 2008; Barnston et al., 1991]. In particular, under east-  
63 erly QBO (EQBO), the EN related anomalous NP low is weaker than in westerly QBO

64 (WQBO), so that a Pacific-North America pattern is apparent mainly under WQBO but  
65 much less so under EQBO. To show this, we composite months that are both EN and  
66 EQBO (hereafter EN/EQBO) and that are both EN and WQBO (hereafter EN/WQBO)  
67 in the reanalysis record (Figure 1a and 1c). The geopotential height anomalies for the  
68 WQBO and EQBO composites differ qualitatively. This previous work motivates our cur-  
69 rent question: how might the QBO affect the troposphere in the NP? In Garfinkel and  
70 Hartmann [2008] (hereafter GH08), we concluded that the difference in EN teleconnec-  
71 tion pattern between EQBO and WQBO “is most likely a random occurrence related to  
72 sampling variability and not a robust relationship.” We now reconsider this conclusion.

73 After discussing the data (Section 2), we show that the results of GH08 and Barnston  
74 et al. [1991] are confirmed (though with much weaker magnitude) by WACCM runs (Sec-  
75 tion 3), indicating that the results of GH08 may be more robust than previously thought.  
76 We then explore possible physical theories for the response of ENSO teleconnections to  
77 the QBO. In Section 4, we present evidence that the QBO might directly affect the NP. In  
78 Section 5, we discuss how this direct effect can alter the climatological mean flow and thus  
79 affect the propagation of the ENSO related Rossby wavetrain. We conclude that while  
80 sampling variability may have had a role in the reduced central Pacific teleconnection for  
81 EN events during EQBO in the observational record, a dynamical argument can be made  
82 for why this relationship should be expected.

## 2. Data

83 The 12 UTC data produced by the ECMWF is used. The ERA-40 dataset is used for  
84 the first 45 years [Uppala et al., 2005], and the analysis is extended by using operational  
85 ECMWF TOGA analysis. All relevant data from the period September 1957 to August

86 2007 are included in this analysis, yielding 50 years of data. For reanalysis, the Niño3.4  
87 index (<http://www.cpc.noaa.gov/data/indices/sstoi.indices>) is used. The QBO  
88 index is the area averaged zonal wind anomaly from 10°S to 10°N at 70hPa (sensitivity  
89 to this definition is discussed in Section 3).

90 Two distinct configurations of WACCM are used to support results from the reanalysis.  
91 One configuration is a coupled seasonal integration and the other is a perpetual January  
92 simulation in which the transient response to QBO winds is investigated. Both configu-  
93 rations of WACCM have 66 vertical levels (a hybrid sigma-vertical coordinate) extending  
94 into the thermosphere, and both configurations have the same QBO relaxation. Between  
95 model layers 0.0026 and 0.08565 (approximately 2.6hPa and 85.66hPa), the winds at the  
96 equator are linearly relaxed towards the specified profile(Figure 2) with a 10 day timescale.  
97 Away from the equator, the linear relaxation timescale increases like a Gaussian distri-  
98 bution with a half width of 10° latitude. Winds are not relaxed poleward of 22° latitude.  
99 At model level 0.1005 (approximately 100.5hPa), the same relaxation is imposed but with  
100 twice the relaxation timescale.

101 In the first configuration, WACCM version 3.5 is run as the atmospheric component of  
102 the NCAR Community Climate System Model [Collins et al., 2006] and interacts with  
103 the land model, a full depth ocean (which generates an ENSO-like phenomenon), and  
104 the sea-ice model(hereafter cWACCM, coupled WACCM). The tropospheric convection  
105 is upgraded compared to version 3.0 to include a new treatment of the dilution of en-  
106 trainment in convection [Neale et al., 2008] and of the convective momentum transport  
107 [Richter and Rasch, 2008], so that the internally generated ENSO is more realistic though  
108 still too vigorous [Neale et al., 2008]. The run used here lasts 126 years and is the same

109 model run used in Garfinkel et al. [2010]. The horizontal resolution is  $1.9^\circ$  latitude by  
110  $2.5^\circ$  longitude. The simulation is a time-slice run with chemical composition correspond-  
111 ing to 1995, and the time-dependent QBO is imposed as prescribed by the Climate-  
112 Chemistry Model Evaluation Activity ([http://www.pa.op.dlr.de/CCMVal/Forcings/](http://www.pa.op.dlr.de/CCMVal/Forcings/CCMVal_Forcing_WMO2010.html)  
113 [CCMVal\\_Forcing\\_WMO2010.html](http://www.pa.op.dlr.de/CCMVal/Forcings/CCMVal_Forcing_WMO2010.html)) for the World Meteorological Organization Ozone As-  
114 sessment. For the cWACCM run, the ENSO index is defined as the anomaly in the surface  
115 radiative temperature averaged over the Niño3.4 region (in other WACCM runs the dif-  
116 ferences between the surface radiative temperature and sea surface temperatures are less  
117 than 0.1%, suggesting that such an ENSO index is appropriate). The extratropical NP  
118 response to deviations of this index resembles (with similar magnitude) the canonical tele-  
119 connection pattern in the reanalysis, implying that this index is appropriate for studying  
120 how the QBO might affect EN teleconnections in the cWACCM run. The QBO index is  
121 defined the same as for the reanalysis. For both the reanalysis and the cWACCM run,  
122 anomalies are computed as deviations from that calendar month's climatology.

123 In the second configuration of WACCM, WACCM version 3.1.9 [Marsh et al., 2007] is  
124 run with fixed sea surface temperatures (SSTs), land surface and ice, perpetual January  
125 15th radiative forcing, and with interactive chemistry turned off (hereafter fWACCM).  
126 The horizontal resolution is  $4^\circ$  latitude by  $5^\circ$  longitude. The fWACCM runs are initialized  
127 by first running WACCM with the full seasonal cycle for two years. Perpetual January  
128 conditions and EN SSTs (see Figure 1 of Taguchi and Hartmann [2006] for the EN SST  
129 anomalies used) are then imposed, and equatorial stratospheric winds are relaxed to the  
130 climatological equatorial stratospheric winds from May 1953 to April 2007 (dashes in  
131 Figure 2). The model is then run for an additional 10,860 days. The last 10,600 days

132 of this run constitutes case A (Table 1). For case B, we branch off the instantaneous  
133 atmospheric state at the beginning of each of the first 130 months of case A and then  
134 integrate each ensemble member for an additional 112 days. Upon branching, the EQBO  
135 wind profile (solid line in Figure 2) is imposed; because the relaxation timescale for the  
136 QBO winds is no faster than 10 days, the atmosphere can smoothly adjust to the EQBO  
137 equatorial stratospheric profile. We thus generate a 130-member ensemble of the transient  
138 NP response to EQBO under EN conditions. We discuss the transient response in the  
139 first three months rather than the equilibrated steady state response because the transient  
140 response more closely approximates the onset of wintertime in the annual cycle and thus  
141 is more relevant to the observed response. Nevertheless, the difference between case B and  
142 case A in the tropospheric NP does not grow systematically in days 40-112 of the ensemble.  
143 The EQBO wind profile in case B is similar to, though slightly stronger than, a typical  
144 EQBO wind profile (i.e. the winds are within the asterisks of Figure 2 which denote the  
145 5%-95% range of QBO variability of the equatorial winds from May 1953 to April 2007).  
146 Unlike real EQBO wind profiles, the case B profile relaxes to climatological easterlies in  
147 the upper stratosphere; preliminary results from a similar run but with realistic upper  
148 stratospheric westerlies qualitatively agree with the results shown here. Any differences  
149 between case A and case B in the midlatitudes or in the troposphere are part of the  
150 response to the EQBO relaxation, rather than due to the underlying forcing. For all three  
151 data sources, significance is determined by a 2 tailed Student-t difference of means test.

### 3. El-Niño under WQBO and EQBO

152 EN's NP wintertime teleconnections differ by QBO phase in both the cWACCM run  
153 and the reanalysis data, extending the results in GH08 for reanalysis. To show this, we

154 composite months that are both EN and EQBO (hereafter EN/EQBO) and that are both  
155 EN and WQBO (hereafter EN/WQBO) for both the reanalysis data and the cWACCM  
156 run. Months between December and March with the ENSO index exceeding 0.65C are  
157 classified as EN, and months with QBO index exceeding  $\pm 2\text{m/s}$  are classified as EQBO or  
158 WQBO. The difference in 300hPa height anomalies between the composites is taken (see  
159 Figure 3a-b). The difference in the NP between the two composites is significant in both  
160 data sources and peaks at over 40m in cWACCM and over 100m in the reanalysis. The  
161 difference between EN and climatology during EQBO in reanalysis data looks qualitatively  
162 different from the same difference during WQBO (see Figure 1a and 1c).

163 We now describe tests of the robustness of this observational result before seeking a  
164 physical explanation for its existence. The minimum criteria necessary for a month to  
165 be included in a composite was varied, and sensitivity to defining the QBO index at  
166 70hPa as opposed to 50hPa was explored, for the reanalysis and the cWACCM run (see  
167 Table 2). For the reanalysis, the central NP low is significantly deeper under WQBO  
168 so long as the composites are of a meaningful size. For the cWACCM run, however, the  
169 difference between QBO phase loses significance as only a smaller number of more extreme  
170 EN or QBO events is considered. The difference between EN/EQBO and EN/WQBO  
171 is significant for a QBO defined at 50hPa as well. The average Niño3.4 index for the  
172 months in the reanalysis EN/WQBO composite (1.48C) is higher than the average Niño3.4  
173 index for the months in the reanalysis EN/EQBO composite (1.16C). Using the observed  
174 linear relationship between Niño3.4 and NP height, we estimate that the 0.32C difference  
175 between the EN/EQBO composite and EN/WQBO composite in Niño3.4 would result in a  
176 12m difference in NP height, which is less than 15% of the difference in NP height between

177 the EN/EQBO composite and EN/WQBO composite. (Nonlinearity in the observed  
178 relationship between NP height and Niño3.4 does not alter this relative unimportance.)  
179 Furthermore, the average Niño3.4 index in the cWACCM run is higher for the EN/EQBO  
180 composite, and yet the structure of the response is similar, if smaller, than the observed  
181 response. Only a small part of the observed difference between EQBO and WQBO may  
182 be due to the different strengthened EN events included in the composites.

183 Additional tests of the robustness were performed but details are excluded for brevity.  
184 The difference between EN/EQBO and EN/WQBO is robust to compositing an equal  
185 number of extreme WQBO and EQBO months. The distribution of the members of  
186 the EQBO and WQBO composites among the different wintertime calendar months is  
187 nearly equal, so the observed difference between EN/WQBO and EN/EQBO is not due  
188 to aliasing of the seasonal cycle of EN teleconnections. As for the composites in GH08, the  
189 EN/EQBO months occur earlier in the reanalysis record than the EN/WQBO months,  
190 but the cWACCM run has no externally imposed trends yet still exhibits the same weaker  
191 teleconnection in EN/EQBO relative to EN/WQBO. Results are qualitatively similar  
192 when using the Niño3 or Niño4 index instead of the Niño3.4. The weaker teleconnection  
193 pattern in EN/EQBO is robust.

194 The robustness of the reanalysis result is also supported by the fWACCM runs. The  
195 300hPa height field after the introduction of EQBO winds(case B) is subtracted from the  
196 300hPa height in the control case (case A) to illustrate the altered NP response to EN  
197 with and without EQBO. Figure 4 shows the difference in the second and third months  
198 after the EQBO relaxation is turned on. By the second month(Figure 4a), the NP low  
199 significantly differs between case A and B, and by the third month(Figure 4b), pattern

200 agreement with the reanalysis (Figure 3a,c) is strongly suggestive of common underlying  
201 dynamics. Both fWACCM cases share identical SSTs yet they differ in the NP. Like the  
202 cWACCM run, the fWACCM runs show a much weaker difference than the reanalysis.

### 3.1. Potential Pathways

203 We now address the mechanisms that may cause the QBO to influence the EN response.  
204 We envision three possible mechanisms. The first pathway through which the QBO  
205 could affect EN teleconnections is by directly affecting divergent outflow from anoma-  
206 lous convection. Figure 1(b,d) shows the divergence anomalies and the anomalous di-  
207 vergent component of the wind for the EN/EQBO and EN/WQBO composites averaged  
208 over the 200hPa-300hPa levels. They are qualitatively similar in the Tropics but not  
209 outside of the deep Tropics. The area averaged divergence from 150hPa-250hPa, 2.5S-  
210 2.5N, 170°E-150°W for the months in the EN/WQBO composite ( $2.5 \times 10^{-6} s^{-1}$ ) is slightly  
211 larger than for the months in the EN/EQBO composite ( $2.0 \times 10^{-6} s^{-1}$ ), consistent with  
212 the slightly stronger EN events that happen to fall in this composite in reanalysis. Linear  
213 regression implies that the  $0.5 \times 10^{-6} s^{-1}$  difference between the EN/EQBO composite and  
214 EN/WQBO composite in divergence would result in a 12m difference in NP height (i.e.  
215  $\alpha$  in NP' =  $\alpha$  div' peaks at 2.3e7ms), less than 15% of the observed difference. Though  
216 differences in tropical convective outflow may contribute to the observed difference be-  
217 tween the EN/EQBO composite and EN/WQBO composite, they seem modest relative to  
218 the large difference in extratropical response. We also examined the Rossby wave source  
219 and found that the Rossby wave source in the reanalysis differs mainly outside the deep  
220 Tropics (like in GH08). The similarity between Figure 1b and 1d in the Tropics, and the  
221 agreement between the cWACCM run, the fWACCM run, and reanalysis in Figure 3 and

222 4, suggest that variation in the structure or intensity of the sampled EN events are not  
223 the explanation for the observed extratropical response to the QBO.

224 The second possibility is that EQBO weakens the NP low directly, independent of any  
225 other perturbation in the system. Thus, the weakened NP response to EN in EQBO  
226 relative to WQBO may have nothing to do with EN and its teleconnections per se. This  
227 direct pathway is discussed in section 4. The third pathway we envision is that once the  
228 QBO affects the Pacific wind field, it can modulate how Rossby waves propagate out of  
229 the Tropics into the extratropics and the extratropical growth. This indirect pathway is  
230 discussed in Section 5.

#### 4. Direct “Effect” of the QBO on the North Pacific

231 We now discuss the possibility of the QBO directly affecting the NP circulation. Com-  
232 posites of 300hPa height anomalies during EQBO and WQBO in the reanalysis and the  
233 cWACCM run show that heights are significantly lower in the NP during WQBO relative  
234 to EQBO(see Figure 5). EN might have a robustly weaker effect on the NP under EQBO  
235 in part because EQBO seems to have a direct effect on the NP. Garfinkel et al. [2010]  
236 found no correlation between height anomalies at 55°N, 175°E and the QBO, but the  
237 QBO is correlated with height farther to the south and east. Nevertheless, the direct  
238 “effect”, as estimated from Figure 5, seems to explain less than half of the difference seen  
239 in Figure 3.

240 The robustness of this result is examined by varying the minimum criteria for classi-  
241 fication of a month as either WQBO or EQBO, by taking an equal number of the most  
242 extreme WQBO and EQBO months, and also by excluding EN months; our results are  
243 not qualitatively changed. Agreement between the cWACCM run and the reanalysis sup-

244 ports the reality of the QBO effect on the troposphere in the NP. Nevertheless, future  
245 work with more idealized models is certainly needed to better understand the mechanism  
246 whereby the QBO can influence the troposphere in the way that these observations and  
247 simulations suggest that it does.

248 In Section 5 we discuss a complementary, indirect, mechanism by which QBO related  
249 zonal wind anomalies in the tropospheric Pacific can affect an ENSO related wave train. In  
250 preparation for discussion of the indirect pathway, we discuss the tropospheric response in  
251 zonal wind to the QBO. Figures 6a and 6b show the difference in Pacific basin zonal wind  
252 anomalies between the EQBO and WQBO composites in the reanalysis and the cWACCM  
253 run. In the troposphere, zonal wind is anomalously westerly near  $35^{\circ}\text{N}$ , with easterly  
254 anomalies in the deep Tropical Pacific and high latitudes, during WQBO compared to  
255 EQBO (consistent with Crooks and Gray [2005] and Haigh et al. [2005]). The reanalysis  
256 and the cWACCM run show a qualitatively similar response to the QBO. These anomalies  
257 are largely in geostrophic balance with the anomalous height in Figure 5. We now show  
258 how such zonal wind anomalies affect a Rossby wave propagating out of the Tropics.

## 5. Modeling the effect of the QBO on the extratropical response to El-Niño

259 The QBO, by varying the background state in the Pacific, can affect a wave train  
260 propagating from the tropical Pacific into the North Pacific. To show this, we linearize  
261 a shallow water model about many idealized background states and then study how a  
262 common tropical vorticity source affects the extratropical circulation for each background  
263 state. A shallow water model is capable of resolving the relevant Rossby wave dynamics  
264 without undue complication, and is thus an appropriate simplified model of this dynamical  
265 process. See Hartmann and Maloney [2001] for a description of the model used; all model

266 parameters are identical to Hartmann and Maloney [2001] except here an equivalent depth  
 267 of 9.2km is used. We first examine idealized background states, and then relate our results  
 268 to the background states observed in WQBO and EQBO.

### 5.1. Idealized Background States

269 An ensemble of background wind states is created by adding idealized wind anomalies  
 270 to the climatological zonal wind. The idealized anomalies are easterly/westerly anoma-  
 271 lies located at 15°N ( $\Delta U_{15} = A \exp\left(\frac{-(\phi-15)}{10}\right)^2 \exp\left(\frac{-(\lambda-180)}{55}\right)^2$ ) and at 35°N ( $\Delta U_{35} =$   
 272  $A \exp\left(\frac{-(\phi-35)}{10}\right)^2 \exp\left(\frac{-(\lambda-180)}{55}\right)^2$ ;  $\phi$  and  $\lambda$  are latitude and longitude in degrees respec-  
 273 tively and A is the amplitude of the perturbation). Amplitudes of  $\pm 2\text{m/s}$ ,  $\pm 4\text{m/s}$ ,  $\pm 6\text{m/s}$ ,  
 274  $\pm 8\text{m/s}$ , and  $\pm 12\text{m/s}$  of the idealized perturbation are tested. These perturbations are  
 275 then added to the 300hPa climatological winds in each month between December and  
 276 February, thus creating our ensemble of background states (results were similar for 200hPa  
 277 winds).

278 In order to approximate the vorticity source associated with anomalous ENSO convec-  
 279 tion, a vorticity source described by  $S(\lambda, \phi, t) = 10^{-7} \cos\left((t-1)\frac{2\pi}{100}\right) \exp\left(\left(\frac{-(\phi-15)}{10}\right)^2\right) \exp\left(\left(\frac{-(\lambda-170)}{60}\right)^2\right)$   
 280 is imposed. This equation describes an oscillating vorticity source with period of 100 days,  
 281 decaying exponentially away from 15°N and 170°E. We examine the last 200 days of a 300  
 282 day run, when the anomalies respond periodically to the imposed forcing. We search for  
 283 when the peak NP response occurs relative to the peak in the vorticity source (typically  
 284 10-20 days later). The height anomalies for the three days surrounding this day for each  
 285 peak of the vorticity source are grouped together. The peak response days in the model  
 286 run with an easterly perturbation are then compared to the peak response days of the run  
 287 with a westerly perturbation. The responses for all the wintertime months are then aver-

288 aged together. We thus examine whether our idealized perturbations to the background  
 289 winds affect the wintertime NP response to the tropical vorticity anomaly.

290 Enhanced easterlies at 15°N or westerlies at 35°N (the observed response during EQBO  
 291 relative to WQBO in Section 4) weaken the NP height response. A similar idealized per-  
 292 turbation near 60°N was found to have little effect on the NP response. To explore this fur-  
 293 ther, a perturbation which has *both* westerlies(easterlies) at 35°N and easterlies(westerlies)  
 294 at 15°N

295  $(\Delta U_{15,35} = A \left( \exp \left( \frac{-(\phi-15)}{10} \right)^2 - \exp \left( \frac{-(\phi-35)}{10} \right)^2 \right) \exp \left( \frac{-(\lambda-180)}{55} \right)^2)$  is added onto each win-  
 296 ter months climatology, and the model is linearized about these states. The response for  
 297 each calendar month from December through February is then averaged. Figure 7A-D  
 298 shows the height anomalies generated by the tropical vorticity anomaly for a  $\pm 2\text{m/s}$  and  
 299  $\pm 6\text{m/s}$  amplitude perturbation with a 6 day drag timescale. In the EQBO-like cases  
 300 (panels A and B) a weaker response is seen as compared to the WQBO-like cases(panels  
 301 C and D), with the effect on the NP response intensifying for larger amplitude idealized  
 302 perturbations. The model does not accurately capture the observed location of the NP  
 303 low, however.

304 The weakened NP response under EQBO to the vorticity forcing is robust to varying  
 305 the model parameters. Moving the vorticity source deeper into the Tropics to 5°N, further  
 306 north to 25°N, or further east to 170°W, has little effect on which background state best  
 307 leads to a stronger wavetrain. Adding a weak secondary vorticity source near the Maritime  
 308 Continent also has little effect on which background state leads to a stronger NP response.  
 309 The response to a 20 or 50 day period vorticity source was weaker but qualitatively  
 310 similar to the source shown here. The response to a steady(i.e. non-periodic) source is

311 stronger, and the difference between WQBO-like and EQBO-like background states is  
 312 larger, than for the oscillating source shown here. The response is slightly weaker when  
 313 the central latitude of the zonal wind perturbation is shifted away from 15°N and 35°N;  
 314 the response is also weakened when the perturbation is more zonally confined. Many  
 315 different drag coefficients were tested to ensure that the difference between EQBO-like  
 316 and WQBO-like states is not sensitive to the drag coefficient. Each wintertime calendar  
 317 months' individual response to the vorticity source, as well as the the response when the  
 318 perturbations are added onto the March and November background state, is weaker for  
 319 the EQBO-like perturbation. Even though we cannot quantitatively extrapolate from  
 320 these model results to the real atmosphere, an EQBO-like background state should lead  
 321 to a weaker NP response than a WQBO-like background state.

## 5.2. Underlying Dynamics of the Shallow Water Model

322 We now explain how the idealized perturbations affect the NP growth of the anomalies.  
 323 We first examine the Pacific sector eddy kinetic energy budget over a complete cycle of  
 324 the tropical vorticity source(i.e. Simmons et al. [1983]). Eddy kinetic energy generated  
 325 by the tropical vorticity source initially propagates northward. As the eddies encounter  
 326 the background state's vorticity gradient at the southern flank of the subtropical jet, the  
 327  $[u'v' \frac{\partial u_0}{\partial y}]$  ( $u_0$  is the zonal wind of the background state about which we linearize, and  $[x]$   
 328 is an average of the response over each of the wintertime months) term of the kinetic  
 329 energy equation leads to much stronger growth of the anomaly if the vorticity gradient is  
 330 enhanced(see Figure 7E-H for the average of the wintertime months'  $[u'v' \frac{\partial u_0}{\partial y}]$  for  $\pm 2\text{m/s}$   
 331 and  $\pm 6\text{m/s}$  amplitude perturbations). The  $[u'v' \frac{\partial u_0}{\partial y}]$  term is of primary importance, rela-  
 332 tive to the other terms in the energy budget, in explaining the difference in extratropical

333 response between the various runs(not shown). The modified anomaly then propagates  
 334 into the NP; the net result is a stronger NP response to WQBO-like background states  
 335 than EQBO-like background states.

336 We also examine the growth of enstrophy and the budget of wave activity density(WAD,  
 337 i.e. Vallis [2006] p.298). For brevity, one case of a WQBO-like background state is  
 338 compared to one case of an EQBO-like background state; other cases are similar. We first  
 339 discuss the budget for a zonally symmetric(WAD arguments are only valid for zonally  
 340 symmetric background states) WQBO-like case. The vorticity source near 15N imposes  
 341  $\overline{q'^2}$  ( $\overline{X}$  denotes a zonal average) anomalies, thus generating  $\frac{\overline{q'^2}}{2\frac{\partial\overline{q_0}}{\partial y}}$  (WAD) in this region(e.g.  
 342 solid line in Figure 8a-b). The local eddy flux of potential vorticity( $\overline{v'q'}$ ) increases WAD  
 343 near 30°N and decreases it near the vorticity source at 15°N(e.g. solid line in Figure 8d),  
 344 while linear drag damps anomalies everywhere.  $\frac{\partial\overline{q_0}}{\partial y}$  is small near 15N relative to its value  
 345 near the subtropical jet(e.g. solid line in Figure 8c). Thus, as the WAD generated near  
 346 15N encounters regions of larger  $\frac{\partial\overline{q_0}}{\partial y}$  near the subtropical jet, enstrophy must increase near  
 347 the subtropical jet to balance the larger  $\frac{\partial\overline{q_0}}{\partial y}$ .

348 A zonally symmetric EQBO-like zonal wind perturbations changes this budget by af-  
 349 fecting the structure of  $\frac{\partial\overline{q_0}}{\partial y}$  between 10°N and 30°N. An EQBO-like perturbation increases  
 350  $\frac{\partial\overline{q_0}}{\partial y}$  near the vorticity source (and reduces it near the subtropical jet) so that a given vor-  
 351 ticity anomaly generates less  $\frac{\overline{q'^2}}{2\frac{\partial\overline{q_0}}{\partial y}}$ . This reduced  $\frac{\overline{q'^2}}{2\frac{\partial\overline{q_0}}{\partial y}}$  leads to a smaller enstrophy anomaly  
 352 near the subtropical jet relative to the case where an WQBO-like perturbation had been  
 353 imposed. The weaker enstrophy anomaly directly leads to a weaker NP height response  
 354 to the same tropical vorticity forcing. A stronger Pacific jet and an expanded region of

355 tropical easterly anomalies thus lead to a stronger NP response by requiring more energy  
 356 conversion from the basic state to the growing enstrophy anomaly.

357 Wave activity density arguments are only strictly valid for zonally averaged anomalies,  
 358 while our interest is primarily in NP growth. To analyze what regions are responsible for  
 359 the WAD response, the Pacific sector (120°E to 120°W) contributions to  $\frac{\overline{q'^2}}{2\frac{\partial \bar{q}_0}{\partial y}}$ ,  $\overline{v'q'}$ , and  $\overline{q'^2}$   
 360 are plotted in Figure 8 (asterisks and triangles). Pacific sector variability dominates the  
 361 WAD and enstrophy, justifying the relevance of a WAD budget analysis for the growth  
 362 of regional NP anomalies. By modifying the background PV gradient, background wind  
 363 anomalies mimicking the tropospheric response to EQBO weaken the NP response to our  
 364 vorticity forcing. Though our model lacks some dynamical processes of relevance to the  
 365 atmosphere (i.e. we expect that baroclinic eddies will positively feedback onto the anomaly  
 366 and affect the precise location of the NP low), we expect that the underlying dynamics  
 367 are still relevant, and perhaps dominant.

### 5.3. Realistic Background States

368 We now test whether the results from our idealized perturbations are relevant to realistic  
 369 QBO wind perturbations. The wind perturbations from our composites in Section 4 are  
 370 added onto the climatological wind in each wintertime calendar month. The same tropical  
 371 vorticity source is then imposed. The December, January, and February response to the  
 372 vorticity source is averaged, and the ensuing NP signal is shown in Figure 9. The WQBO  
 373 background state leads to a stronger NP response than the EQBO background state.  
 374 We find this is true for a background state corresponding to each calendar month from  
 375 December to March, and for all drag timescales tested. Even though our model is too

376 simplistic to be applied quantitatively, our results indicate that the QBO can indirectly  
377 affect EN teleconnections by modifying the background state that Rossby waves encounter.

378 Because the NP response in the linearized shallow water is sensitive to the latitude at  
379 which zonal wind perturbations are added, we wish to highlight the nature of the Pa-  
380 cific sector tropospheric response to the QBO. One might naively have assumed that the  
381 tropospheric response to the QBO in the Pacific resembles the response to anomalies in  
382 the lower stratospheric vortex, as the vortex tends to be stronger under WQBO than  
383 EQBO. We thus demonstrate that the Pacific sector tropospheric response to the QBO  
384 differs from the Pacific sector tropospheric response to anomalies in the lower stratospheric  
385 polar vortex. The difference in Pacific sector winds between months with strong lower  
386 stratospheric vortices and weak lower stratospheric polar vortices is plotted in Figure  
387 6c(STRONG-WEAK; composite definition in caption). Zonal wind in the troposphere in  
388 the Pacific increases north of the climatological tropospheric jet position and decreases  
389 near the climatological tropospheric jet position(i.e. like the positive phase of the North-  
390 ern Annular Mode(NAM)). A comparison of 6a to Figure 6c shows how disparate the  
391 tropospheric Pacific response to the QBO is from the response to anomalies in the vortex.  
392 The response to the QBO is only NAM-like in the Atlantic basin [Boer and Hamilton,  
393 2008], where the zonal wind is enhanced north of its climatological maximum during  
394 WQBO and south of its climatological position during EQBO.

395 This difference between the Pacific sector tropospheric response to the QBO and to  
396 anomalies of the vortex is important for the results from the linearized shallow water  
397 model. A perturbation to the climatological Pacific wind distribution that mimics the  
398 positive phase of the NAM (which is associated with a strong vortex and thus might be

399 connected to WQBO) leads to a *weaker* tropospheric NP response, based on the analysis in  
400 Section 5.1-5.2. In contrast, we find that the NP response to a vorticity source is actually  
401 *stronger* under WQBO. Because the QBO at 70hPa does not lead to a NAM response in  
402 the Pacific, Rossby wave trains are of larger magnitude in the NP under WQBO in our  
403 shallow water model.

## 6. Summary and Discussion

404 Both reanalysis data and WACCM simulations suggest that the North Pacific response  
405 to El Niño is weaker under EQBO than WQBO, though the difference between EQBO  
406 than WQBO is much smaller in the WACCM simulations than in the reanalysis. Some  
407 of this weakened response to El Niño may be a direct result of the QBO. The QBO, by  
408 modifying the background conditions experienced by a Rossby wave train propagating  
409 out of the Tropics, can then indirectly affect the extratropical response to El Niño. To  
410 explore this indirect effect, a shallow water model is linearized about both EQBO-like and  
411 WQBO-like background flows. Perturbations in zonal wind that mimic the tropospheric  
412 response to EQBO modify the background state's PV gradient and lead to a reduction in  
413 the North Pacific response to a deep tropical vorticity source, similar to the effect in both  
414 WACCM and the observations. The tropospheric zonal wind response to the QBO in the  
415 Tropics and subtropics may thus provide a physical explanation for some of the observed  
416 relationship between QBO and the response in the North Pacific to EN.

417 Sampling variability or convective variability in the deep Tropics cannot be excluded as  
418 a contributor to the observed dependence of the extratropical EN response on the phase  
419 of the QBO. Some of the discrepancy between the reanalysis and the cWACCM run in  
420 the magnitude of the difference is likely due to differences in convection and sampling

421 variability. We thus cannot be certain that the observed magnitude of the difference  
422 in geopotential height at 300hPa in the reanalysis between EQBO than WQBO will be  
423 repeated in the future. Nevertheless, the physical mechanism demonstrated here and the  
424 consistency between reanalysis data and WACCM simulations suggest that the mechanism  
425 we have described is important.

426 The difference between EQBO and WQBO is smaller under La-Niña conditions than  
427 El Niño conditions in both the reanalysis and the cWACCM run. We would expect this  
428 asymmetry from the direct effect discussed in section 4, though we would expect the  
429 indirect effect discussed in section 5 to be more symmetrical.

430 The results of this study could have important implications for predictability of El Niño  
431 teleconnections. Since the QBO is largely periodic and bimodal[Garfinkel and Hartmann,  
432 2007], a potentially more accurate seasonal forecast of the Central and Northwestern  
433 Pacific response to developing EN conditions could be gained by incorporating the QBO.  
434 A more thorough test of each link in our chain of logic is currently ongoing. In particular,  
435 we are investigating the response to the QBO in the Pacific sector in the absence of  
436 anomalous El Niño SST anomalies.

437 Finally, the results of the linearized shallow water model are potentially relevant to the  
438 seasonal cycle of El Niño teleconnections, to altered El Niño teleconnections in a chang-  
439 ing climate, and to altered El Niño teleconnections under anomalous polar stratospheric  
440 vortices. The strength and position of the North Pacific tropospheric jet differs among  
441 the calendar months and will change as CO<sub>2</sub> increases[Meehl et al., 2006]. In wintertime  
442 (and especially January and February), the Pacific jet is stronger and has larger merid-  
443 ional gradients of the background potential vorticity. In our model, such a background jet

444 leads to a stronger North Pacific teleconnection as compared to the background profile in  
445 March. Connecting the results and physical mechanism from our linearized shallow water  
446 model to the observed seasonal cycle of El Niño teleconnections, to intra-winter variabil-  
447 ity of El Niño teleconnections(e.g. Frederiksen and Branstator [2005]), to changes in El  
448 Niño teleconnections under altered stratospheric polar vortices[Bell et al., 2009], and to  
449 changes in future El Niño teleconnections(e.g. Meehl et al. [2006]; Müller and Roeckner  
450 [2008] and Schneider et al. [2009]), merits future attention.

451 **Acknowledgments.** This work was supported by the Climate Dynamics Program of  
452 the National Science Foundation under grant ATM 0409075. We thank Jinkui Zhu for  
453 help with the shallow water model runs, Peter Rhines for our many helpful conversations,  
454 Fabrizio Sassi for providing the data from the WACCM 3.5 run, the developers at NCAR  
455 for the use of WACCM 3.1.9, and Marc L. Michelsen for assisting our WACCM 3.1.9 runs.  
456 Finally, we appreciate our anonymous reviewers whose comments have led to an improved  
457 manuscript.

## References

- 458 M. P. Baldwin and T. J. Dunkerton. Propagation of the Arctic Oscillation from the  
459 stratosphere to the troposphere. *J. Geophys. Res.*, 104(D24):30937–30946, 1999.
- 460 M. P. Baldwin, L. J. Gray, T. J. Dunkerton, K. Hamilton, P. H. Haynes, W. J. Randel,  
461 J. R. Holton, M. J. Alexander, I. Hirota, T. Horinouchi, D. B. A. Jones, J. S. Kinner-  
462 sley, C. Marquardt, K. Sato, and M. Takahashi. The Quasi-Biennial Oscillation. *Rev.*  
463 *Geophys.*, 39(2):179–229, 2001.

- 464 A. G. Barnston, R. E. Livezey, and M. S. Halpert. Modulation of Southern Oscillation-  
465 Northern Hemisphere mid-winter climate relationships by the QBO. *J. Clim.*, 4:203–217,  
466 1991.
- 467 C. J. Bell, L. J. Gray, A. J. Charlton-Perez, M. M. Joshi, and A. A. Scaife. Stratospheric  
468 Communication of El Niño Teleconnections to European Winter. *Journal of Climate*,  
469 22:4083–+, 2009. doi: 10.1175/2009JCLI2717.1.
- 470 G. J. Boer and K. Hamilton. QBO influence on extratropical predictive skill. *Climate*  
471 *Dynamics*, 31:987–1000, December 2008. doi: 10.1007/s00382-008-0379-5.
- 472 G. Branstator. The maintenance of low-frequency atmospheric anomalies. *J. Atmos. Sci.*,  
473 49:1924–1946, 1992.
- 474 C. C. Collimore, D. W. Martin, M. H. Hitchman, A. Huesmann, and D. E. Waliser. On  
475 the relationship between the QBO and tropical deep convection. *J. Clim.*, 16(15), 2003.  
476 doi: 10.1175/1520-0442(2003).
- 477 W. D. Collins, C. M. Bitz, M. L. Blackmon, G. B. Bonan, C. S. Bretherton, J. A. Carton,  
478 P. Chang, S. C. Doney, J. J. Hack, T. B. Henderson, J. T. Kiehl, W. G. Large, D. S.  
479 McKenna, B. D. Santer, and R.D. Smith. The community climate system model version  
480 3 (CCSM3). *J. Clim.*, 19:2122–2143, 2006.
- 481 K. Coughlin and K.-K. Tung. QBO Signal found at the Extratropical Surface through  
482 Northern Annular Modes. *Geophys. Res. Lett.*, 28:4563–4566, 2001. doi: 10.1029/  
483 2001GL013565.
- 484 S. A. Crooks and L. J. Gray. Characterization of the 11-year solar signal using a multiple  
485 regression analysis of the ERA-40 dataset. *J. Clim.*, 18:996–1015, 2005.

- 486 S. B. Feldstein. Fundamental mechanisms of the growth and decay of the PNA tele-  
487 connection pattern. *Quart. J. Roy. Meteorol. Soc.*, 128:775–796, April 2002. doi:  
488 10.1256/0035900021643683.
- 489 C. Franzke and S. B. Feldstein. The continuum and dynamics of northern hemisphere  
490 teleconnection patterns. *J. Atmos. Sci.*, 62:3250–3267, September 2005. doi: 10.1175/  
491 JAS3536.1.
- 492 J. S. Frederiksen and G. Branstator. Seasonal Variability of Teleconnection Patterns.  
493 *Journal of Atmospheric Sciences*, 62:1346–1365, May 2005. doi: 10.1175/JAS3405.1.
- 494 C. I. Garfinkel and D. L. Hartmann. Effects of the El-Nino Southern Oscillation and the  
495 Quasi-Biennial Oscillation on polar temperatures in the stratosphere. *J. Geophys. Res.-*  
496 *Atmos.*, 112:D19112, 2007. doi: 10.1029/2007JD008481.
- 497 C. I. Garfinkel and D. L. Hartmann. Different ENSO teleconnections and their effects  
498 on the stratospheric polar vortex. *J. Geophys. Res.- Atmos.*, 113, 2008. doi: 10.1029/  
499 2008JD009920.
- 500 C. I. Garfinkel, D. L. Hartmann, and F. Sassi. Tropospheric precursors of anomalous  
501 northern hemisphere stratospheric polar vortices. *J. Clim.*, accepted, 2010.
- 502 J. D. Haigh, M. Blackburn, and R. Day. The response of tropospheric circulation to  
503 perturbations in lower-stratospheric temperature. *J. Clim.*, 18:3672–3685, 2005. doi:  
504 10.1175/JCLI3472.1.
- 505 D. L. Hartmann and E. D. Maloney. The Madden–Julian Oscillation, barotropic dynamics,  
506 and North Pacific tropical cyclone formation. Part II: Stochastic barotropic modeling.  
507 *J. Atmos. Sci.*, 58:2559–2570, 2001.

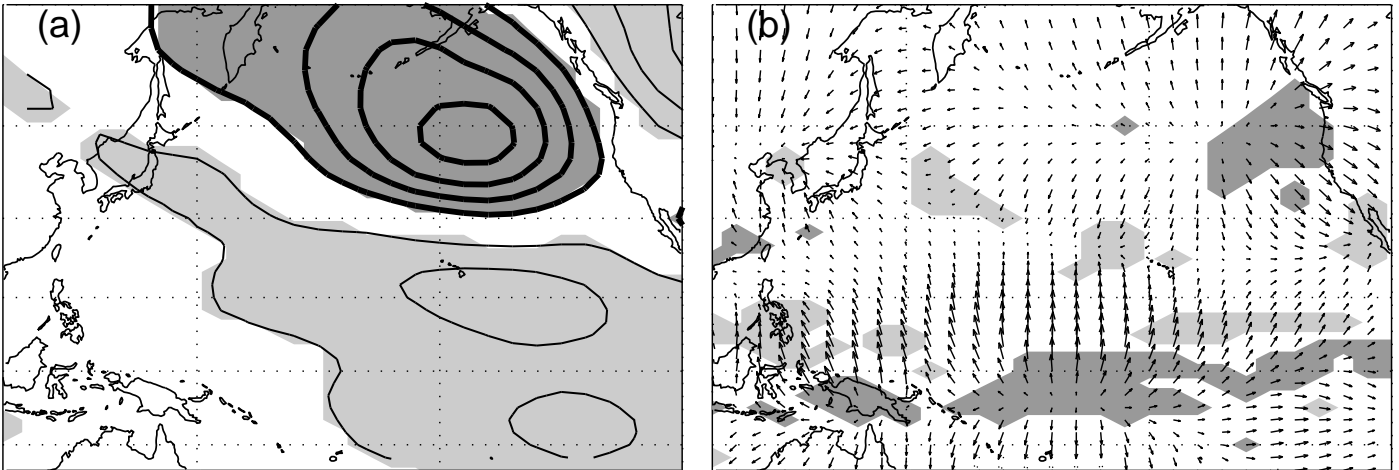
- 508 I. M. Held, S. W. Lyons, , and S. Nigam. Transients and the extratropical response to El  
509 Nino. *J. Atmos. Sci.*, 46(1):163–174, 1989.
- 510 C.-H. Ho, H.-S. Kim, J.-H. Jeong, and S.-W. Son. Influence of stratospheric quasi-biennial  
511 oscillation on tropical cyclone tracks in the western North Pacific. *Geophys. Res. Lett.*,  
512 36, March 2009. doi: 10.1029/2009GL037163.
- 513 J. R. Holton and H. C. Tan. The influence of the equatorial Quasi-Biennial Oscillation  
514 on the global circulation at 50mb. *J. Atmos. Sci.*, 1980.
- 515 B. J. Hoskins and D. Karoly. The steady linear response of a spherical atmosphere to  
516 thermal and orographic forcing. *J. Atmos. Sci.*, 38:1179–1196, 1981.
- 517 V. Limpasuvan, D. W. J. Thompson, and D. L. Hartmann. The life cycle of the Northern  
518 Hemisphere sudden stratospheric warmings. *J. Clim.*, 17:2584–2596, 2004.
- 519 D. Marsh, R. R. Garcia, D. E. Kinnison, B. A. Boville, F. Sassi, S. C. Solomon, and  
520 K. Matthes. Modeling the whole atmosphere response to solar cycle changes in radiative  
521 and geomagnetic forcing. *J. Geophys. Res.*, 112, 2007. doi: 10.1029/2006JD008306.
- 522 G. A. Meehl, H. Teng, and G. Branstator. Future changes of El Niño in two global  
523 coupled climate models. *Climate Dynamics*, 26:549–566, May 2006. doi: 10.1007/  
524 s00382-005-0098-0.
- 525 W. A. Müller and E. Roeckner. ENSO teleconnections in projections of future climate  
526 in ECHAM5/MPI-OM. *Climate Dynamics*, 31:533–549, October 2008. doi: 10.1007/  
527 s00382-007-0357-3.
- 528 R. B. Neale, J. H. Richter, and M. Jochum. The impact of convection on ENSO: From a  
529 delayed oscillator to a series of events. *J. Clim.*, 21:5904–5924, 2008.

- 530 L. M. Polvani and P. J. Kushner. Tropospheric response to stratospheric perturbations  
531 in a relatively simple general circulation model. *Geophys. Res. Lett.*, 29, 2002. doi:  
532 10.129/2001GL014284.
- 533 J. H. Richter and P. J. Rasch. Effects of convective momentum transport on the at-  
534 mospheric circulation in the Community Atmosphere Model, version 3. *J. Clim.*, 21:  
535 1487–1499, 2008.
- 536 A. Ruzmaikin, J. Feynman, X. Jiang, and Y. L. Yung. Extratropical signature of  
537 the Quasi-Biennial Oscillation. *J. Geophys. Res.*, 110:D1111, 2005. doi: 10.1029/  
538 2004JD005382.
- 539 P. D. Sardeshmukh and B. J. Hoskins. The generation of global rotational flow by steady  
540 idealized tropical divergence. *J. Atmos. Sci.*, 45:1228–1251, 1988.
- 541 E. K. Schneider, M. J. Fennessy, and J. L. Kinter. A Statistical-Dynamical Estimate of  
542 Winter ENSO Teleconnections in a Future Climate. *Journal of Climate*, 22:6624, 2009.  
543 doi: 10.1175/2009JCLI3147.1.
- 544 A. Simmons, J. M. Wallace, and G. Branstator. Barotropic wave propagation and insta-  
545 bility, and atmospheric teleconnection patterns. *J. Atmos. Sci.*, 40:1363–1392, 1983.
- 546 M. Taguchi and D. L. Hartmann. Increased occurrence of stratospheric sudden warming  
547 during El Niño as simulated by WAACM. *J. Clim.*, 19:324–332, 2006. doi: 10.1175/  
548 JCLI3655.1.
- 549 M. Ting and P. D. Sardeshmukh. Factors determining the extratropical response to  
550 equatorial diabatic heating anomalies. *J. Atmos. Sci.*, 50:907–918, 1993.
- 551 S. M. Uppala, P. W. Kållberg, A. J. Simmons, U. Andrae, V. da Costa Bechtold, M. Fior-  
552 ino, J. K. Gibson, J. Haseler, A. Hernandez, G. A. Kelly, X. Li, K. Onogi, S. Saari-

553 nen, N. Sokka, R.P. Allan, E. Andersson, K. Arpe, M. A. Balmaseda, A. C. M. Bel-  
554 jaars, L. van de Berg, J. Bidlot, N. Bormann, S. Caires, F. Chevallier, A. Dethof,  
555 M. Dragosavac, M. Fisher, M. Fuentes, S. Hagemann, E. Hólm, B. J. Hoskins, L. Isak-  
556 sen, P. A. E. M. Janssen, R. Jenne, A. P. McNally, J. F. Mahfouf, J. J. Morcrette, N. A.  
557 Rayner, R. W. Saunders, P. Simon, A. Sterl, K. E. Trenberth, A. Untch, D. Vasiljevic,  
558 P. Viterbo, and J. Woollen. The ERA-40 reanalysis. *Quart. J. Roy. Meteorol. Soc.*,  
559 2005.

560 G. K. Vallis. *Atmospheric and Oceanic Fluid Dynamics: Fundamentals and Large-Scale*  
561 *Circulation*. Cambridge University Press, 2006.

## EN and WQBO



## EN and EQBO

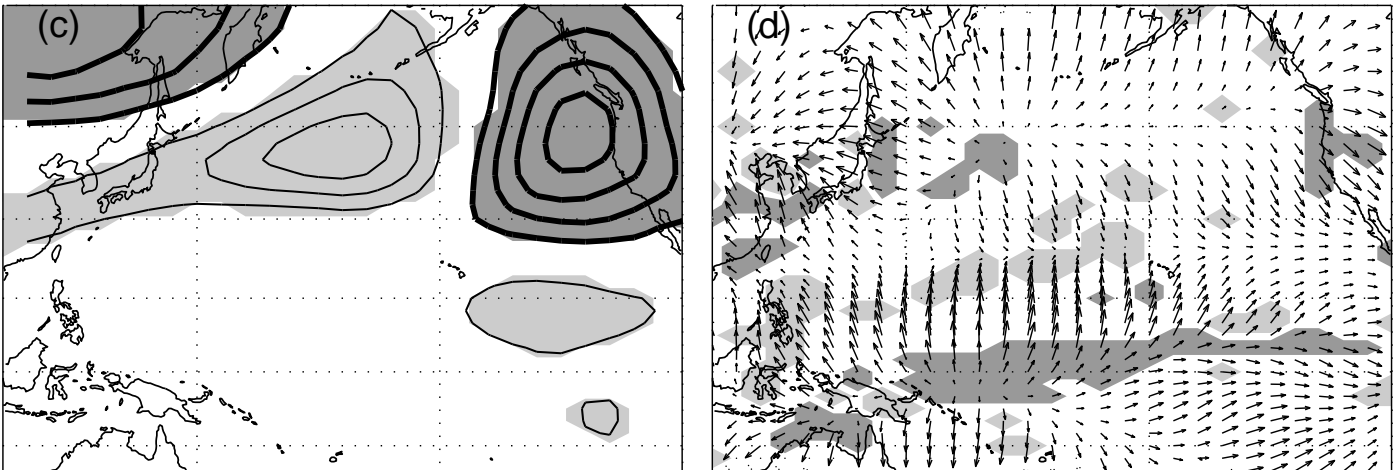


**Figure 1.** Geopotential height anomalies at 300hPa(a,c), divergence anomalies, and the anomalous divergent component of the wind averaged over 200hPa-300hPa(b,d) for the EN/WQBO(a,b) and EN/EQBO(c,d) composites from reanalysis. Months with the ENSO index exceeding 0.65C are classified as EN, and months with anomalous tropical zonal wind at 70hPa exceeding  $\pm 2\text{m/s}$  are classified as EQBO or WQBO. For (b) and (d), regions with divergence exceeding  $10^{-6}\text{s}^{-1}$  are shaded; divergent regions are shaded dark gray and convergent regions light gray. The velocity vectors are scaled identically between panels (b) and (d), and the longest arrow present denotes a wind speed of  $3.08 \frac{\text{m}}{\text{s}}$ . For (a) and (c), the contour interval is 20m, the zero contour is omitted, negative contours are thicker, and negative(positive) regions shaded dark(light) gray.

Idealized fWACCM runs

case	SSTs	Trop. Strat. wind evolution	length
A	EN	steady climatological	10,600 days
B	EN	branched EQBO	130 112 day runs

**Table 1.** The different idealized WACCM runs considered for uncovering the tropospheric signal of the QBO.

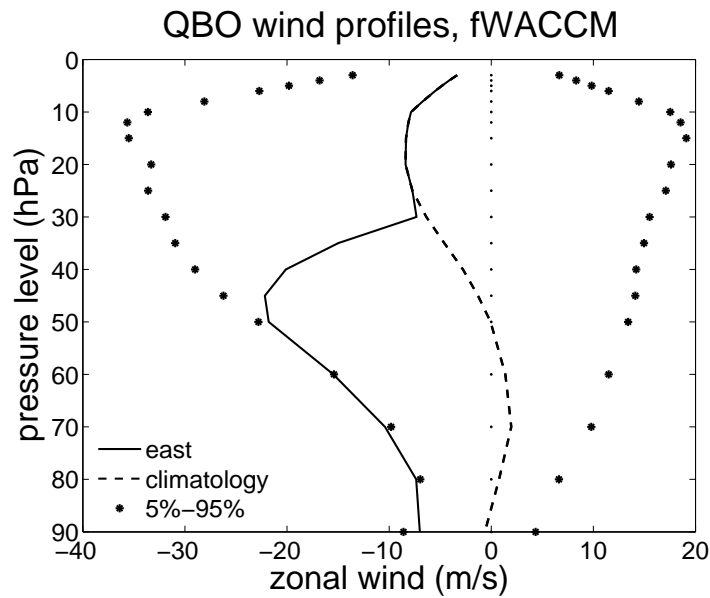


**Figure 2.** The QBO profiles relaxed towards in the fWACCM runs, along with the 5%-95% range of QBO variability of the equatorial winds from May 1953 to April 2007.

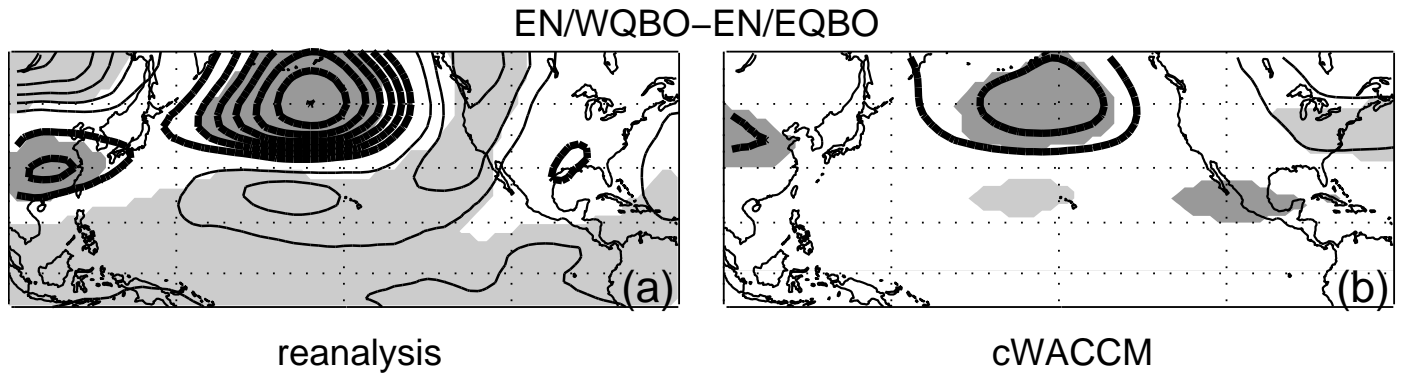


**Figure 3.** Difference in 300 hPa EN height anomalies between WQBO and EQBO (i.e.  $EN/WQBO-EN/EQBO$ ) in DJFM. Significantly positive(negative) height anomalies at the 95% level are shaded light(dark) gray. (a) is for reanalysis, and (b) for cWACCM. The same composite definition in Figure 1 is used for (a) and (b). There are 14(42) EQBO/EN and 23(92) WQBO/EN months in the reanalysis(cWACCM) composites. Contour interval is 20m.

## Robustness of Difference in NP height between EN/EQBO and EN/WQBO

(a)	N3.4 thresh.	$ \text{QBO}_{50}  > 2.5\text{m/s}$	$ \text{QBO}_{50}  > 5\text{m/s}$	$ \text{QBO}_{50}  > 7.5\text{m/s}$
	0.65	<b>-120.3</b> , 26, 13; <b>-46.6</b> , 107, 59	<b>-135.0</b> , 24, 12; <b>-35.5</b> , 87, 44	<b>-140.6</b> , 18, 11; -33.5, 55, 37
	0.95	<b>-101.4</b> , 20, 9; <b>-42.1</b> , 91, 52	<b>-121.4</b> , 18, 8; -28.9, 74, 39	<b>-130.9</b> , 13, 7; -19.9, 48, 33
	1.25	-88.3, 13, 5; <b>-35.2</b> , 84, 45	<b>-129.7</b> , 12, 4; -25.8, 69, 33	<b>-169.1</b> , 8, 3; -21.2, 44, 27
(b)	N3.4 thresh.	$ \text{QBO}_{70}  > 1\text{m/s}$	$ \text{QBO}_{70}  > 2\text{m/s}$	$ \text{QBO}_{70}  > 3\text{m/s}$
	0.65C	<b>-120.3</b> , 29, 15; <b>-35.6</b> , 114, 49	<b>-114.9</b> , 23, 14; <b>-43.3</b> , 92, 42	<b>-131.7</b> , 15, 14; -29.7, 65, 34
	0.95C	<b>-117.1</b> , 23, 9; -27.9, 98, 43	<b>-108.8</b> , 19, 9; -27.8, 79, 37	<b>-131.3</b> , 12, 9; -19.5, 55, 29
	1.25C	<b>-120.0</b> , 14, 4; -23.3, 92, 37	-93.4, 11, 4; -23.8, 73, 32	<b>-115.2</b> , 7, 4; -16.8, 50, 26

**Table 2.** Robustness of the difference in Central North Pacific geopotential height

between EN/EQBO and EN/WQBO (i.e. EN/WQBO-EN/EQBO) for a wide range of composite definitions. The first number in each cell is the difference in the reanalysis, the second is the size of the reanalysis EN/WQBO composite and the third is the size of the reanalysis EN/EQBO composite; the fourth, fifth, and sixth numbers are identical but for the cWACCM run. Differences significant at the 95% level are bolded. The equatorial zonal wind at 50hPa is used in (a) and the equatorial zonal wind at 70hPa is used in (b).

For each case, the largest difference in the region 155°E-180°E, 42.5N-50N is shown.

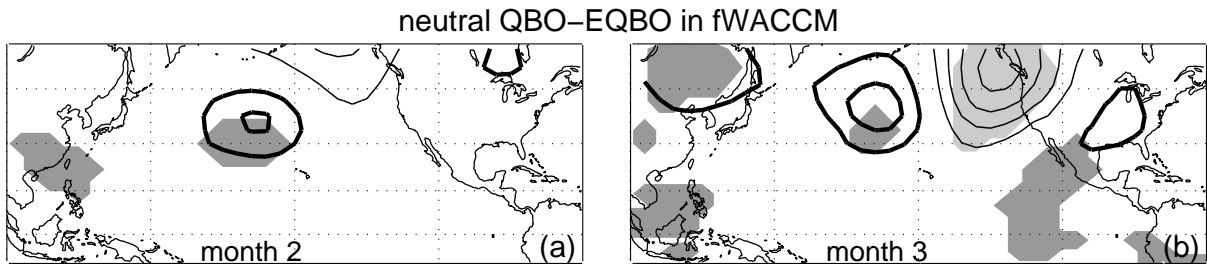


**Figure 4.** Monthly averaged 300hPa Height in case A minus that in case B (i.e. EN/noQBO-EN/EQBO) the second month(a) and third month(b) after the EQBO forcing is switched on in the fWACCM runs. Positive(negative) anomalies significant at the 95% level are shaded light(dark) gray. Contour interval is 10m.

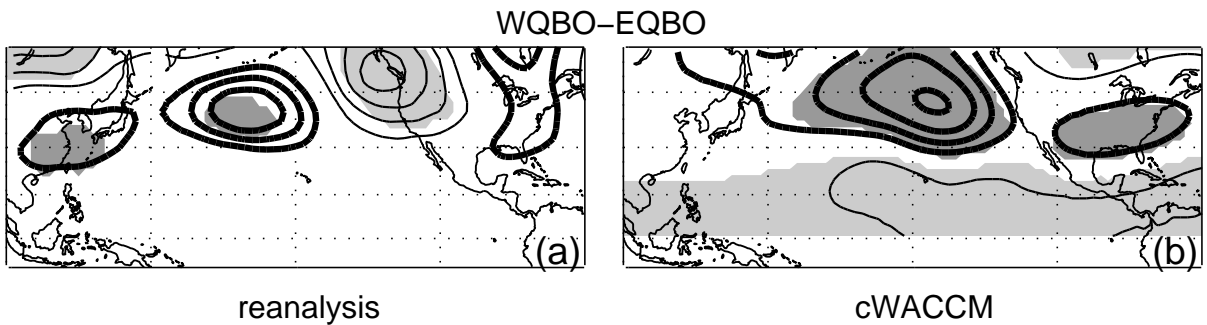


**Figure 5.** Composites of height anomalies at 300hPa in WQBO relative to EQBO(i.e. WQBO-EQBO) in the reanalysis (a) and the cWACCM run (b) in NDJF. Positive(negative) anomalies significant at the 95% level are shaded light(dark) gray. Months with anomalous tropical zonal wind at 70hPa exceeding 2m/s are classified as EQBO or WQBO. The reanalysis (cWACCM) WQBO composite has 95(226) months, and the reanalysis (cWACCM) EQBO composite has 65(161) months. Contour interval is 10m. Significance shading is not extended south of the equator.

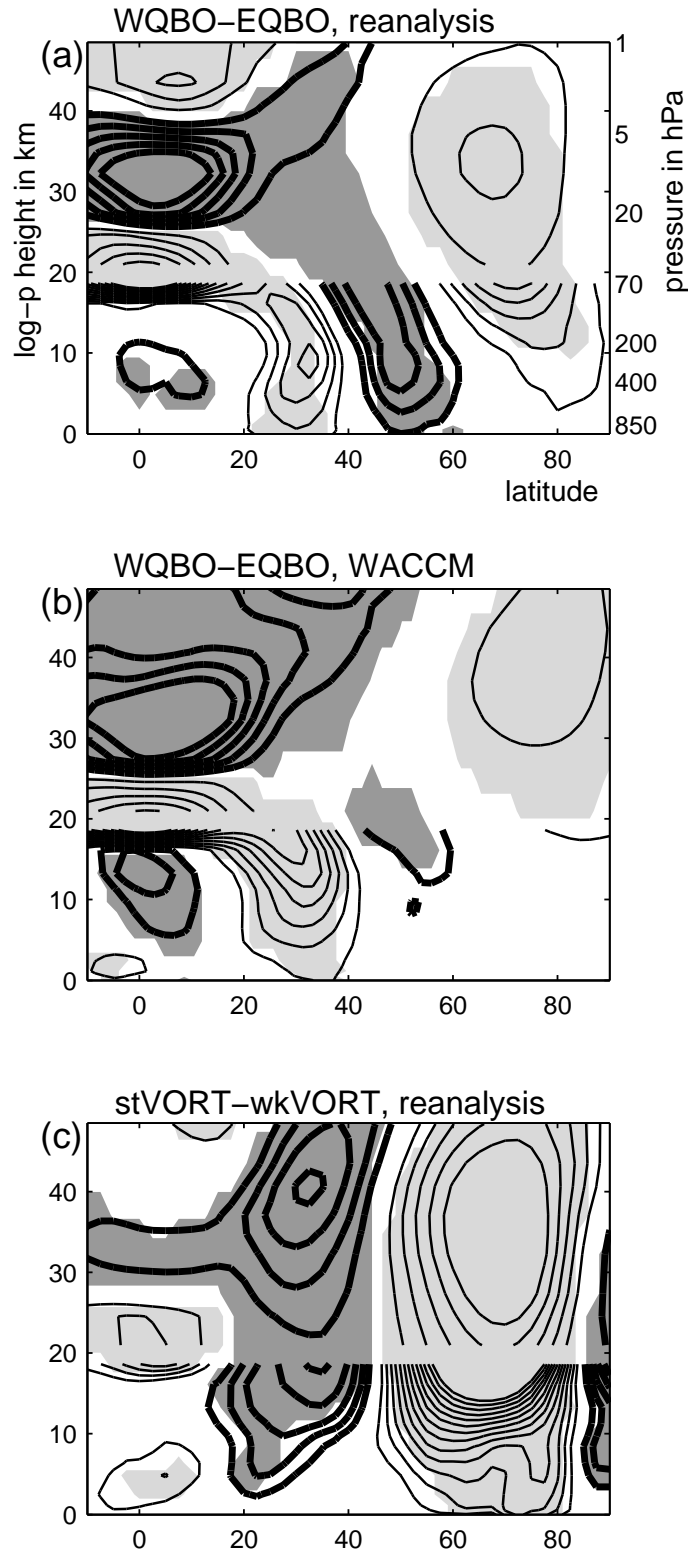


**Figure 6.** Pacific sector cross sections of zonal wind anomalies in the reanalysis and the cWACCM run for NDJF. Positive(negative) anomalies significant at the 95% level are shaded light(dark) gray. (a) and (b) are the difference between the two QBO phases(WQBO-EQBO) in the Pacific sector(average from  $160^{\circ}\text{E}$  to  $160^{\circ}\text{W}$ ) in the reanalysis and the cWACCM run respectively. Same composites in Figure 5 are used here. (c) shows the difference in the Pacific sector between strong lower stratospheric vortices and weak lower stratospheric polar vortices(defined as months when height anomalies vertically and area averaged from 70hPa to 150hPa and  $65^{\circ}\text{N}$  and poleward exceed 0.5 standard deviations) in reanalysis. Contour interval is 0.75m/s below 70hPa and 5m/s above.

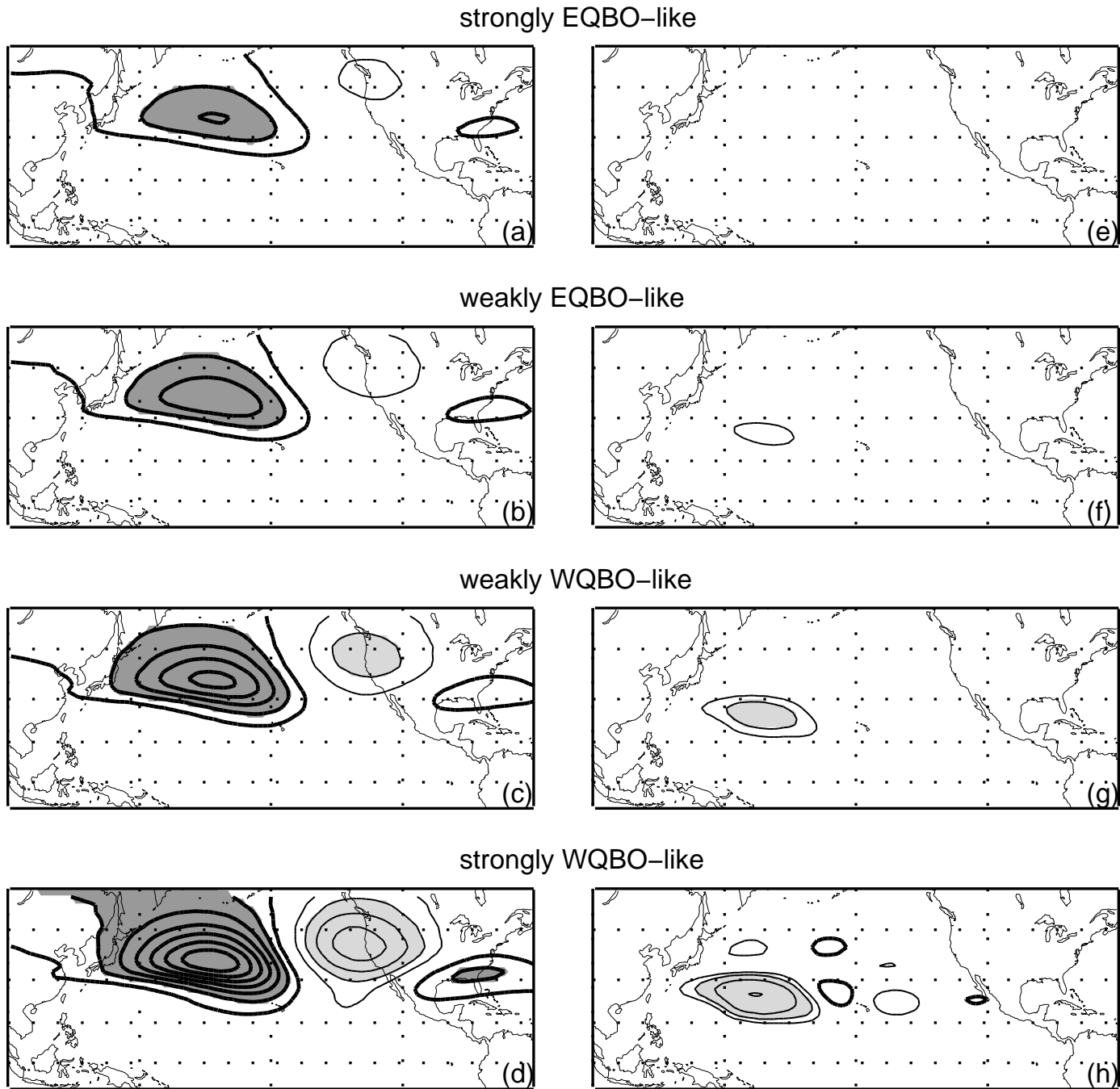


**Figure 7.** Response to an oscillating vorticity anomaly in the deep Tropics in a model linearized about the each winter months' mean state with Gaussian wind anomalies added in the subtropics and deep Tropics. The response in each winter month is then averaged together. A-D are for height anomalies, with a contour interval of 15 meters and regions with negative(positive) height anomalies exceeding 30m shaded dark(light) gray. E-H are for  $[u'v' \frac{\partial u_0}{\partial y}]$ , with contours marked at  $\pm 0.002, \pm 0.004, \pm 0.008, 0.0160, 0.0320 \frac{m^2}{s^2 day}$  and positive anomalies exceeding 0.004m shaded light gray. A(B) and E(F) are for 6m/s (2m/s) deep tropical westerlies and subtropical easterlies, and C(D) and G(H) are for 2m/s (6m/s) deep tropical easterlies and subtropical westerlies.

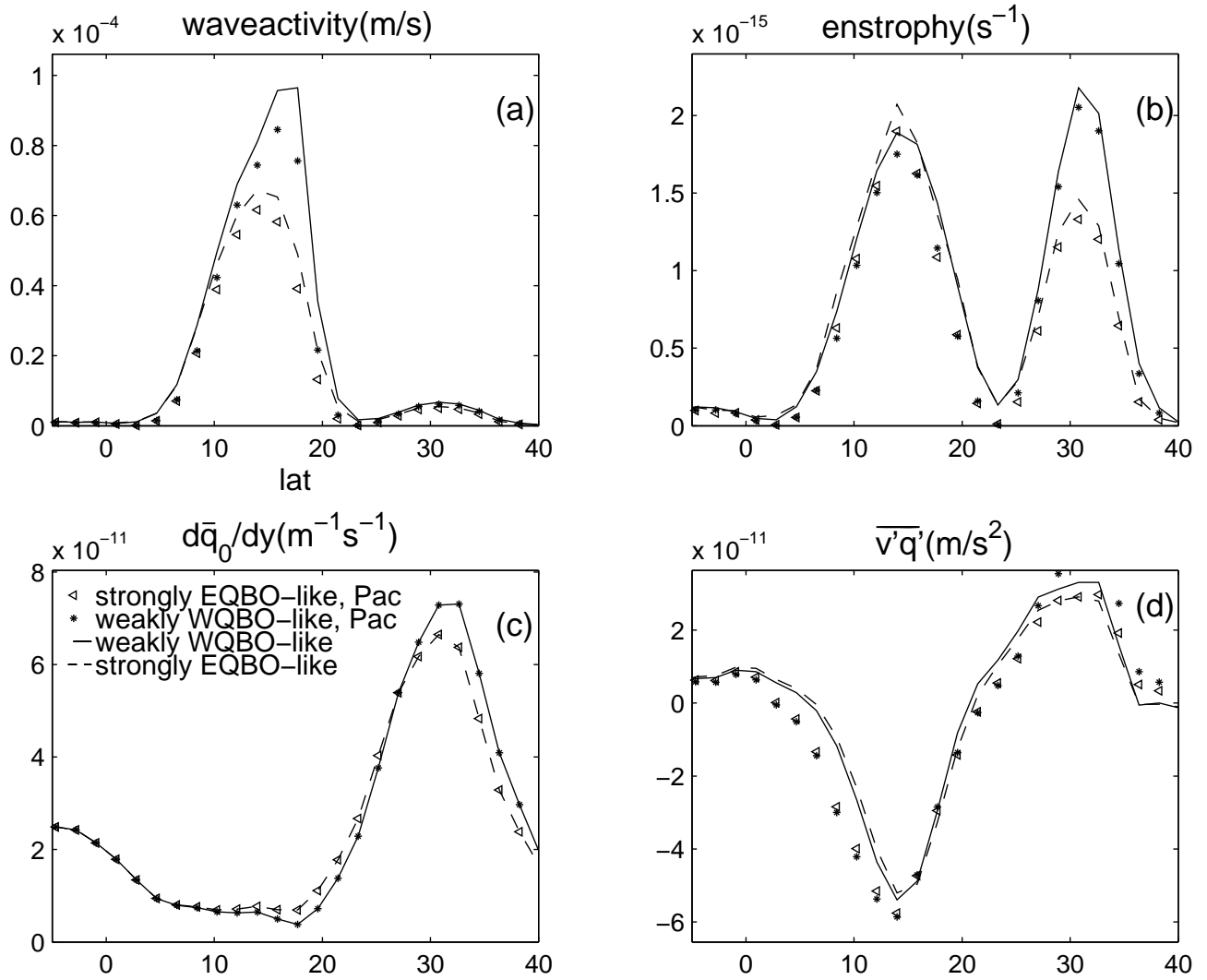


**Figure 8.** Response to an oscillating vorticity anomaly in the deep Tropics for two background states.

Both background states formed by adding a zonally symmetric perturbations to zonally symmetric winds that mimic those in the Pacific ( $130^{\circ}E-170^{\circ}W$ ) in February. Dashed line and triangles are for the 6m/s subtropical easterlies (strongly EQBO-like) case in the zonal average and Pacific sector respectively. Solid line and asterisks are for the 2m/s subtropical westerlies (weakly WQBO-like) case in the zonal average and Pacific sector respectively.

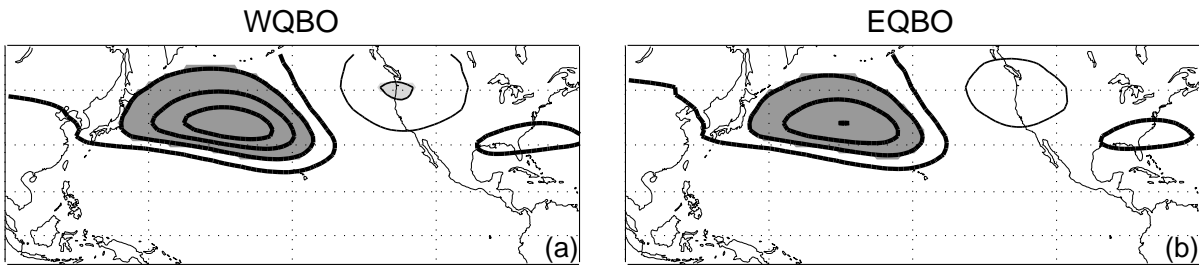


**Figure 9.** Response to an oscillating vorticity anomaly in the Tropics. Model linearized about the EQBO and WQBO wind anomalies added onto the December, January, and February mean state, and the response in each month is then averaged. Contour interval is 15 meters. Regions with negative(positive) height anomalies exceeding 30m are shaded dark(light) gray. The drag timescale is 6 days.